Computational Modelling of Concrete Structures – Bićanić et al. (Eds)
© 2014 Taylor & Francis Group, London, ISBN 978-1-138-00145-9

Microprestress-solidification theory: Modeling of size effect on drying creep

Z.P. Bažant
Department of Civil Engineering, Northwestern University, Evanston, Illinois, USA

P. Havlásek & M. Jirásek
Department of Mechanics, Faculty of Civil Engineering, Czech Technical University in Prague, Czech Republic

ABSTRACT: The microprestress-solidification theory of concrete creep is first recast in a different but equivalent format, which permits elimination of one model parameter without affecting generality of the model and can serve as the basis of an efficient numerical method. The mechanical model is then combined with a moisture transport model and used in finite element simulations of shrinkage and creep of slabs and prisms. Comparison to experimental data reveals that the model can provide good fits of some of thecreep curves from the literature but fails to properly reproduce the experimentally observed size effect on drying creep. The main reason is that the originally postulated equation for microprestress relaxation is too simple and does not cover a full spectrum of relaxation times. This leads to a delay between the humidity changes and the resulting increase of viscosity that contributes to drying creep. A modification which takes into account the instantaneous effects on viscosity by an additional viscousdashpot is outlined and the resulting improvement of the model performance is demonstrated.

1 INTRODUCTION

Mathematical modeling and numerical simulation of time-dependent response of concrete belong to indispensable tools for the design of reliable and durable concrete structures. From the physical point of view, creep and shrinkage are the most important phenomena that need to be taken into account. They are affected by changes of humidity and temperature, which makes the development of a general and realistic model quite complicated.

At sufficiently low stress levels, creep of concrete can be described by models formulated within the framework of linear viscoelasticity with aging. Once the principle of superposition is accepted, the material behavior is uniquely described by the compliance function, J, which reflects the time evolution of strain in a creep test at the unit stress level. For aging materials, it is considered as a function of two arguments: time t, which corresponds to the current age of concrete, and time t', which is the age at the beginning of the creep test.

Many analytical expressions and empirical formulae have been proposed in the literature and in design codes for the approximation of the compliance function based on experimental data and for its prediction from the physical parameters characterizing the concrete and its environment. In this contribution, an advanced model based on the combination of the solidification theory (Bažant & Prasannan 1989a, Bažant & Prasannan 1989b) with the concept of microprestress (Bažant, Hauggaard, Baweja, & Ulm 1997, Bažant, Hauggaard, & Baweja 1997, Bažant, Cusatis, & Cedolin 2004) is adopted. It will be recast in a format that leads to equivalent results but reduces the number of model parameters, which simplifies the identification procedure. The performance of the model will be illustrated by examples, and it will be shown that the effect of specimen size on drying creep can be captured properly only if one of the parameters is set to a nonstandard value, or if the model is modified.

The original Microprestress-Solidification (MPS) theory postulated a nonlinear differential equation governing the evolution of the so-called microprestress, which is an idealized model abstraction that represents large local stress peaks developing in the microstructure of cement paste due to its heterogeneity. Several new model parameters which do not possess a direct physical meaning had to be introduced. In this contribution we present a reformulation of the standard MPS theory with the governing equation rewritten in terms of viscosity, which allows for a reduction of the number of parameters. At constant humidity and temperature, this equation reduces to a very simple form and is integrated exactly even with a basic

numerical algorithm. Under general conditions, a term dependent on the rate of humidity and temperature is activated, and the differential equation becomes nonlinear, but it can still be integrated with a high accuracy based on a closed-form solution for a special case (Jirásek & Havlásek 2014). The evolution of humidity is computed from a nonlinear diffusion equation based on the model of Bažant & Najjar (1971).

The main objectives of the paper are to reformulate the governing equations such that a redundant model parameter is eliminated, to validate the model and identify its parameters by fitting experimental data, to point out a certain deficiency in application to drying creep of specimens of different sizes, and to suggest a modification which may eliminate this deficiency. All numerical computations presented here have been performed using the finite element package OOFEM (Patzák & Bittnar 2001, Patzák 2012), with the original MPS model and its modified version implemented by the present authors.

2 MICROPRESTRESS-SOLIDIFICATION THEORY

The complete constitutive model for creep and shrinkage of concrete can be represented by the rheological scheme shown in Fig. 1. It consists of (i) a non-aging elastic spring, representing instantaneous elastic deformation, (ii) a solidifying Kelvin chain, representing mainly the short-term creep, (iii) an aging dashpot with viscosity dependent on the microprestress, S, representing the long-term creep, (iv) a shrinkage unit, representing volume changes due to drying, and (v) a unit representing thermal expansion. All these units are connected in series, and thus the total strain is the sum of the individual contributions, while the stress transmitted by all units is the same.

According to the solidification theory (Bažant & Prasannan 1989a, Bažant & Prasannan 1989b), aging of concrete is caused by a gradual deposition of new layers of solidified hydration products, which are considered as a non-aging constituent with material properties invariable in time, and the evolution of compliance with age is attributed to the growth of the volume fraction of hydration products. The specific expressions for the non-aging compliance and for the volume growth proposed by Bažant & Baweja (1995), based on fitting of an extensive set of experimental data, lead to the basic compliance function of the B3 model in the form

$$J_b(t,t') = q_1 + q_2 \int_{t'}^{t} \frac{n s^{-m}}{s-t'+(s-t')^{1-n}}\,\mathrm{d}s + q_3 \ln\left[1+(t-t')^n\right] + q_4 \ln\frac{t}{t'} \tag{1}$$

where $n=0.1$, $m=0.5$, and q_1, q_2, q_3 and q_4 are adjustable parameters. The B3 model provides empirical formulae for estimation of these parameters from concrete composition and strength. The first (constant) term in (1) corresponds to the compliance $q_1 = 1/E_0$ of the elastic spring in Fig. 1, the second and third terms to the solidifying viscoelastic material, and the fourth term to a viscous dashpot with age-dependent viscosity

$$\eta(t) = \frac{t}{q_4} \tag{2}$$

The rate of shrinkage strain ε_{sh} at the material point level is assumed to be proportional to the rate of pore relative humidity h, with a proportionality factor denoted as k_{sh}. The effects of temperature and humidity on processes in the microstructure can be described by introducing two transformed time variables: the equivalent age t_e (equivalent hydration period, or "maturity"), which indirectly characterizes the degree of hydration, and the reduced time t_r, characterizing the changes in the rate of bond breakages and restorations on the microstructural level.

In addition to the adjustment of the viscoelastic creep compliance, it is necessary to take into account the effects of temperature and humidity

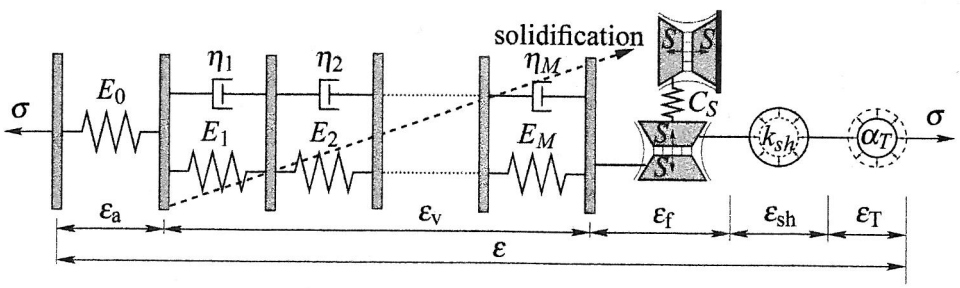

Figure 1. Rheological scheme of the complete hygro-thermo-mechanical model.

on the evolution of the viscous flow. The microprestress-solidification theory (Bažant, Hauggaard, Baweja, & Ulm 1997, Bažant, Hauggaard, & Baweja 1997) replaces the explicit dependence of viscosity η on concrete age t by a dependence on the so-called microprestress, S, which is governed by a separate evolution equation. The microprestress is understood as the stress in the cement paste microstructure generated by large localized volume changes during the hydration process. It builds up at very early stages of microstructure formation and then is gradually reduced by relaxation processes. The microprestress is considered to be much bigger than any stress acting on the macroscopic level, and therefore it is not influenced by the macroscopic stress. Additional microprestress is generated by changes of internal relative humidity and temperature. This is described by the nonlinear differential equation

$$\dot{S} + \psi_S(T,h) c_0 S^p = k_1 \left| \frac{\mathrm{d}(T \ln h)}{\mathrm{d}t} \right| \tag{3}$$

in which the superimposed dot denotes differentiation with respect to time, c_0 and k_1 are constant parameters, p is an exponent usually set equal to 2, and ψ_S is a variable factor that reflects the acceleration of microprestress relaxation at higher temperatures and its deceleration at lower temperatures or lower humidities (compared to the standard conditions).

Owing to the presence of the absolute value operator on the right-hand side of (3), additional microprestress is generated by both drying and wetting, and by both heating and cooling, as suggested by Bažant, Cusatis, & Cedolin (2004). Factor ψ_S is related to yet another transformed time, called the reduced microprestress time, which determines the rate of microprestress relaxation. The dependence of this factor on temperature and humidity is assumed in the form Bažant, Cusatis, & Cedolin 2004

$$\psi_S(T,h) = \exp\left[\frac{Q_S}{k_B}\left(\frac{1}{T_0} - \frac{1}{T}\right)\right] \cdot \left[\alpha_S + (1-\alpha_S) h^2\right] \tag{4}$$

with default parameter values $Q_S/kB = 3000$ K and $\alpha_S \approx 0.1$.

As discussed by Bažant, Hauggaard, Baweja, & Ulm (1997), high microprestress facilitates sliding in the microstructure and thus accelerates creep. Therefore, the viscosity of the dashpot that represents long-term viscous flow is assumed to be increasing with decreasing microprestress. This viscosity acts as a proportionality factor between the flow rate and the stress. The model is described by the equations

$$\sigma = \frac{\eta(S)}{\psi_r(T,h)} \dot{\varepsilon}_f \tag{5}$$

$$\eta(S) = \frac{S^{1-p}}{cp} \tag{6}$$

where ε_f is the viscous strain (i.e., strain in the viscous dashpot in Fig. 1), and ψ_r is a factor that transforms the actual time into the reduced time t_r and is given by a formula similar to (4) but with parameters $Q_r/k_B = 5000$ K and $\alpha_r \approx 0.1$ (Bažant 1995). Equation (6) contains a new parameter c, which is not independent and can be linked to the already introduced parameters. It suffices to impose the requirement that, under standard conditions ($T = T_0$ and $h = 1$) and constant stress, the evolution of the viscous flow strain should be logarithmic and should exactly correspond to the last term of the compliance function (1) of model B3. A simple comparison reveals that

$$cp = (p-1) c_0 q_4 \tag{7}$$

At the same time, we obtain the appropriate initial condition for microprestress, which must supplement differential equation (3). The initial condition reads

$$S(t_0) = \left[(p-1) c_0 t_0\right]^{1/(1-p)} \tag{8}$$

where t_0 is a suitably selected time that precedes (or coincides with) the onset of drying or temperature variations.

For general applications with variable environmental conditions, it is necessary to determine parameters c_0 and k_1 that appear in the microprestress evolution equation (3) and indirectly affect the flow viscosity. The next section will clarify that the stress-strain law actually does not depend on parameters c_0 and k_1 separately but only on their product. The model response is also influenced by parameters α_r and α_S, for which default values have been recommended. As will be shown in Section 5.1, a better agreement with experimental results can be obtained if the default values are adjusted.

3 VISCOSITY EVOLUTION EQUATION

The concept of microprestress is useful for the theoretical justification of evolving viscosity and of the general format of governing equations. On the other hand, the microprestress cannot be directly measured, and a separate calibration of the microprestress relaxation equation (3) and of equation (6) describing the dependence of viscosity

on microprestress is difficult, if not impossible. It turns out that the microprestress can be completely eliminated, and the governing equation can be reformulated in terms of viscosity. The resulting model is then fully equivalent to the original one, but its structure is simplified, the role of model parameters becomes more transparent and the number of relevant parameters is reduced.

From (6) combined with (7) we can express the microprestress in terms of the viscosity as

$$S = [(p-1)c_0 q_4 \eta]^{-1/(p-1)} \tag{9}$$

and differentiation with respect to time leads to

$$\dot{S} = -(c_0 q_4)^{-1/(p-1)}[(p-1)\eta]^{-p/(p-1)}\dot{\eta} \tag{10}$$

Substituting (9)–(10) into (3), we obtain, after some rearrangements,

$$\dot{\eta} + k_1[c_0 q_4 (p-1)^p]^{\frac{1}{p-1}} \left|\frac{\mathrm{d}(T\ln h)}{\mathrm{d}t}\right| \eta^{\frac{p}{p-1}} = \frac{\psi_S}{q_4} \tag{11}$$

For the standard value of parameter $p = 2$, the resulting equation reads

$$\dot{\eta} + k_1 c_0 q_4 \left|\dot{T}\ln h + T\frac{\dot{h}}{h}\right| \eta^2 = \frac{\psi_S}{q_4} \tag{12}$$

This is a nonlinear first-order differential equation for viscosity, which can be solved directly, without resorting to the microprestress. At constant humidity and temperature, the second term on the left-hand side vanishes and the viscosity evolution equation (even for a general value of exponent p) simplifies to

$$\dot{\eta} = \frac{\psi_S}{q_4} \tag{13}$$

At variable temperature or humidity, the second term on the left-hand side of (12) slows down the growth of viscosity and, if sufficiently large, can even lead to a temporary reduction of viscosity.

Reformulation of the governing differential equation in terms of viscosity facilitates the understanding of the role of individual parameters. Parameter p fully determines the exponent $p/(p-1)$ at η in the nonlinear term. Parameters k_1 and c_0 appear only in the expression for the multiplicative factor in the nonlinear term and they can be replaced by one single parameter. Indeed, the values of k_1 and c_0 do not need to be known separately—what matters is only the value of $k_1 c_0^{1/(p-1)}$. For the standard choice of $p = 2$, this means that only the product $k_1 c_0$ matters. If k_1 is multiplied by 10 and c_0 divided by 10, the resulting evolution of viscosity is not affected at all, and the creep flow strain evolves exactly in the same manner as for the original combination of parameters. What changes is only the evolution of microprestress.

Since the microprestress is not directly measurable, parameters k_1 and c_0 cannot be determined separately and optimal fitting based on macroscopically measured variables cannot lead to a unique result. For this reason, it is better to replace k_1 and c_0 by a single parameter which can be uniquely determined. One could of course consider $k_1 c_0^{1/(p-1)}$ as the new single parameter. To avoid units with non-integer exponents (in the general case of p different from 2) and to obtain a parameter with some physical meaning, it is suggested to introduce a parameter μ_S with the dimension of fluidity (reciprocal value of viscosity) and to cast equation (11) in the form

$$\dot{\eta} + \frac{1}{\mu_S T_0}\left|\dot{T}\ln h + T\frac{\dot{h}}{h}\right| (\mu_S \eta)^{\tilde{p}} = \frac{\psi_S}{q_4} \tag{14}$$

where T_0 is the room temperature and $\tilde{p} = p/(p-1)$ is a transformed exponent, introduced for convenience.

A comparison of the second terms in (11) and (14) reveals that

$$\mu_S = c_0 T_0^{p-1} k_1^{p-1} q_4 (p-1)^p \tag{15}$$

This relation provides a link between the original parameters k_1 and c_0 and the new parameter μ_S. For the standard choice $p = 2$, we get $\tilde{p} = 2$ and equations (14)–(15) simplify to

$$\dot{\eta} + \frac{\mu_S}{T_0}\left|\dot{T}\ln h + T\frac{\dot{h}}{h}\right| \eta^2 = \frac{\psi_S}{q_4} \tag{16}$$

$$\mu_S = c_0 T_0 k_1 q_4 \tag{17}$$

The initial condition for viscosity

$$\eta(t_0) = \frac{t_0}{q_4} \tag{18}$$

can be deduced from the initial condition for microprestress (8) combined with relations (6) and (7). Its form is consistent with the fact that, in the absence of drying and at room temperature, the evolution of viscosity should be the same as in model B3, i.e., should be given by (2).

Numerical treatment of equation (14) is discussed in detail by Jirásek & Havlásek (2014), who describe an efficient algorithm for step-by-step integration. After an approximation of time

derivatives by finite differences, the differential equation is converted into a nonlinear algebraic equation, which can be solved iteratively by the Newton method. For the standard exponent $p = 2$, it is possible to construct an exact solution of differential equation (16) with the right-hand side and the coefficient at η^2 replaced by constants. The numerical solution then remains accurate even for large time steps.

4 MOISTURE TRANSPORT

The microprestress-solidification theory takes into account the influence of humidity and temperature on creep at each material point separately (unlike the simplified sectional approach, which averages these effects over the cross section), and thus the distribution of the pore relative humidity h and temperature T in the structure and their evolution in time need to be determined by using appropriate moisture and heat transport models.

For tests performed at constant room temperature, $T = T_0$, only the pore relative humidity has to be calculated. The well-known moisture transport model proposed by Bažant & Najjar (1971) can be used for that purpose. The governing nonlinear diffusion equation reads

$$\dot{h} = \nabla \cdot (C(h) \nabla h) \tag{19}$$

where h is the pore relative humidity, ∇ is the divergence operator, C is the moisture diffusivity [m²/s] and ∇h is the gradient of relative humidity. For concrete and other cementitious materials, the dependence of diffusivity on relative humidity is highly nonlinear. According to (Bažant & Najjar 1971) it can be approximated by

$$C(h) = C_1 \left(\alpha_0 + \frac{1 - \alpha_0}{1 + \left(\frac{1-h}{1-h_c} \right)^r} \right) \tag{20}$$

where C_1 is the moisture diffusivity at full saturation [m²/s], α_0 is the ratio between the minimum diffusivity at very low saturation and maximum diffusivity at full saturation, h_c is a parameter that corresponds to the relative humidity in the middle of the transition between low and high diffusivity, and exponent r controls the shape of that transition. The *fib* Model Code 2010 (Fédération internationale de béton (fib) 2010) recommends the following default values of parameters: $\alpha_0 = 0.05$, $h_c = 0.8$ and $r = 15$. The maximum diffusivity C_1 can be estimated from the mean compressive strength using an empirical formula.

5 SIMULATION OF EXPERIMENTS

5.1 *Variation of temperature and humidity*

The performance of the MPS model under variable temperature and humidity was studied by Havlásek & Jirásek (2012) and Jirásek & Havlásek (2014), who exploited the experimental data of Kommendant, Polivka, & Pirtz (1976), Nasser & Neville (1965) and Fahmi, Polivka, & Bresler (1972). Beside the exponent $\tilde{p}$ with standard value 2, the MPS theory reformulated in terms of viscosity (Eq. 14) uses only one additional parameter, μ_S, which was varied until the best fit with experimental data was obtained. For instance, a really good fit of the first experimental data set of Fahmi, Polivka, & Bresler (1972) (creep of sealed specimens subjected to an increase of temperature applied in two steps) was obtained for $\mu_S = 875 \times 10^{-6}/(\text{MPa} \cdot \text{day})$; see Fig. 2. The agreement is very satisfactory, except for the last interval, which corresponds to unloading. It is worth noting that the thermally induced part of creep accounts for more than a half of the total strain (compare the experimental data with the dashed curve in Fig. 2).

In order to simulate the creep evolution for the second experimental data set of Fahmi, Polivka, & Bresler (1972) (drying and one thermal cycle) it was first necessary to calibrate parameters of the Bažant-Najjar model for moisture diffusion. Since the distribution of relative humidity across the section was not measured, the parameters had to be identified indirectly from the time evolution of shrinkage and thermal strains of the unloaded companion specimen (Fig. 3). Parameters α_0, h_c and r were set to their default values

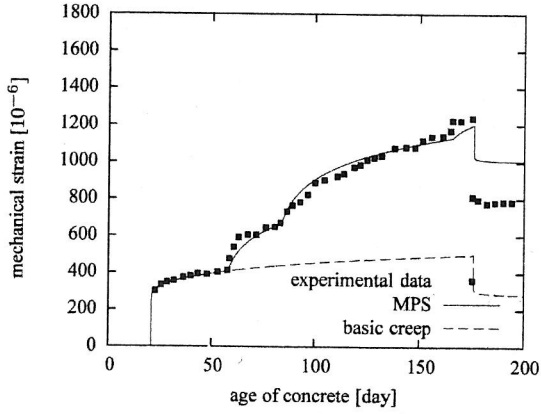

Figure 2. **Mechanical strain** evolution for **sealed** specimens, with pore relative humidity assumed to be 98%, loaded by compressive stress 6.27 MPa at age $t' = 21$ days, with ambient temperature increased from 23°C to 47°C at age 58 days and to 60°C at age 84 days and reduced back to 23°C at age 166 days, and unloaded at 187 days.

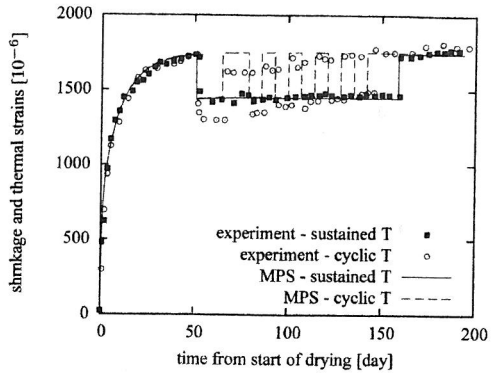

Figure 3. **Shrinkage and thermal strain** evolution for specimens drying from age $t_0 = 18$ days at 50% ambient relative humidity.

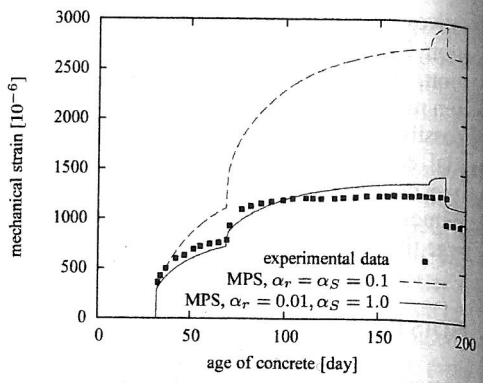

Figure 4. **Mechanical strain** evolution for specimens drying from age $t_0 = 18$ days at 50% ambient relative humidity, loaded by compressive stress 6.27 MPa at age $t' = 32$ days, with ambient temperature increased from 23°C to 60°C at age 69 days and reduced back to 23°C at age 177 days, and unloaded at 187 days.

according to *fib* recommendations; see Section 4. The best agreement was reached with maximum diffusivity $C_1 = 25$ mm^2/day, shrinkage parameter $k_{sh} = 0.0039$, and coefficient of thermal expansion $\alpha_T = 8 \times 10^{-6}$/K. Unfortunately, with default values of the other parameters, the value of μ_S calibrated on the first data set could not be used to fit the second experimental data set, because it would have led to a gross overestimation of the creep (see the dashed curve in Fig. 4). However, it is possible to accurately reproduce the experimental data without changing μ_S if the values of parameters α_r and α_S are adjusted to 0.01 and 1.0 respectively (solid curve in Fig. 4). These parameters control the effect of reduced humidity on the rate of bond breakages and the rate of microprestress relaxation, and the modification has no effect on the response of sealed specimens in Fig. 2.

Jirásek & Havlásek (2014) also showed that if the specimen is subjected to several cycles of elevated temperature, the effect of temperature variations on creep is overestimated by the standard MPS theory, and they proposed a modification of the microprestress source term that reduces this spurious effect.

5.2 *Size effect on creep*

Another extensive set of experimental data that can be used for evaluation of the MPS model was reported by Bryant & Vadhanavikkit (1987), who measured basic and drying creep and shrinkage on slabs and prisms of different sizes. Let us first present the calibration procedure, which starts from the parameters of the basic creep compliance function. Parameter $q_4 = 6.5 \cdot 10^{-6}$/MPa controlling the long-time creep is determined using the empirical formula of the B3 model, based on the aggregate/cement ratio. Parameters q_1 to q_3 were initially estimated using the empirical formulae based on the

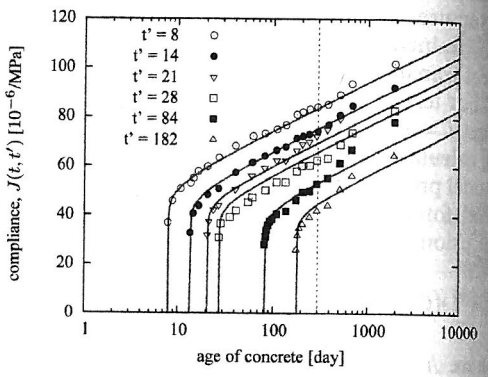

Figure 5. Basic creep compliance curves measured by Bryant and Vadhanavikkit (1987) for different ages at loading t' and their fits by the B3 model (the dashed line indicates the approximate time of sealing failure in the experiment).

compressive strength and composition but they had to be adjusted to get a good agreement with the experimental data; see Fig. 5. Their optimized values are $q_1 = 9 \cdot 10^{-6}$/MPa, $q_2 = 75 \cdot 10^{-6}$/MPa and $q_3 = 28 \cdot 10^{-6}$/MPa.

Next, it is necessary to fit four parameters of the Bažant & Najjar (1971) moisture transport model, and also the shrinkage coefficient k_{sh} and the fluidity parameter μ_S. Moreover, the complete model used here takes into account cracking by a simple approach based on damage mechanics, with two fundamental parameters (tensile strength and fracture energy).

It has been found that the results are quite insensitive to the exact values of the crack model parameters, as long as they remain within a reasonable range characteristic of the given concrete class. What really matters is whether cracking is taken into account or not. If it is neglected, the

shrinkage deformation grows faster and reaches a higher final value. On the other hand the compliance is higher if cracking is considered; the reason is that the compliance is computed as a difference between the total and shrinkage strains divided by the compressive stress. Therefore a smaller value of the shrinkage strain is subtracted from the total strain and this results in a higher compliance.

Since no information on humidity profiles or water loss in the experiments of Bryant & Vadhanavikkit (1987) is available, the parameters of the Bažant & Najjar (1971) moisture transport model are again estimated from the measured shrinkage, using the assumption of proportionality between the humidity change and shrinkage strain at the material point level. The approximate values of parameters have been obtained by inverse analysis, based on fitting of the experimentally measured shrinkage curves. A trial-and-error procedure has been used to calibrate the Bažant-Najjar diffusion parameters and the shrinkage coefficient k_{sh} on shrinkage data of a 150 mm thick slab (thick curve, second from the left in Fig. 6). The optimized values are $C_1 = 40$ mm^2/day, $\alpha_0 = 0.18$, $h_c = 0.75$, $r = 10$ and $k_{sh} = 0.00195$. The other, thinner curves show that with these parameters the agreement with all the experimental shrinkage data is excellent, except for the last data point in the 200 mm, 300 mm and 400 mm series. Regarding the fluidity parameter μ_S, a tentatively estimated value is used in this set of simulations, because shrinkage development is not sensitive to that parameter.

The fluidity parameter μ_S, which controls the magnitude of drying creep, is then calibrated to give the best possible agreement with the experimental measurements of creep on a 150 mm thick drying slab (Fig. 7). With $\mu_S = 5 \cdot 10^{-6}$/(MPa·day),

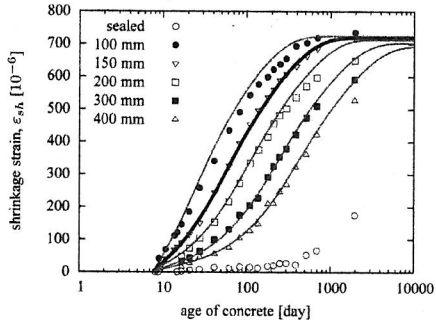

Figure 6. **Shrinkage** curves measured by Bryant and Vadhanavikkit (1987) for drying **slabs** of different thicknesses D and their fits by a numerical model based on Bažant-Najjar moisture transport model combined with the MPS theory and assumption of proportionality between shrinkage strain and humidity change; onset of drying at $t_0 = 8$ days.

the final increase of compliance due to drying is captured correctly, but the shape of the curve differs from the experimental data. The acceleration of compliance growth predicted by the model is delayed with respect to the experimental data. If the same value of μ_S is used for prediction of creep compliance functions for specimens of other sizes, a more dramatic delay is observed; see Fig. 8. But what is even more striking is that the contribution of drying creep is incorrectly scaled with specimen size. According to the experiments, the effect of drying on creep of larger slabs is weaker. This is logical, because the halftime of the drying process increases with increasing specimen size and in the limit of an infinitely thick slab the compliance should be the same as under sealed conditions. In contrast to that, the MPS model predicts a dramatic long-time increase of compliance for large specimens.

Interestingly, a parametric study has revealed that the size effect on drying creep can be controled by

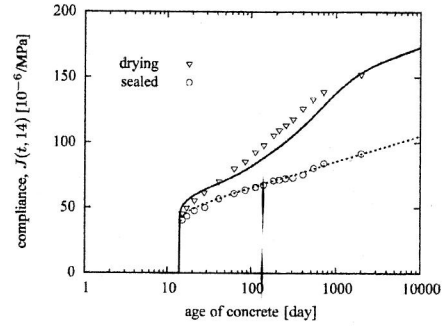

Figure 7. **Creep** compliance curve measured by Bryant and Vadhanavikkit (1987) on a **drying slab** of thickness $D = 150$ mm and its fit by the **MPS model** with parameters $\mu_S = 5 \cdot 10^{-6}$/(MPa·day) and $\tilde{p} = 2$; onset of drying at $t_0 = 8$ days, loading applied at $t' = 14$ days.

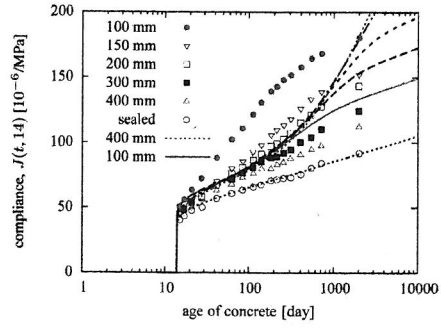

Figure 8. **Creep** compliance curves measured by Bryant and Vadhanavikkit (1987) on **drying slabs** of different thicknesses D and their fits by the **MPS model** with parameters $\mu_S = 5 \cdot 10^{-6}$/(MPa·day) and $\tilde{p} = 2$; onset of drying at $t_0 = 8$ days, loading applied at $t' = 14$ days.

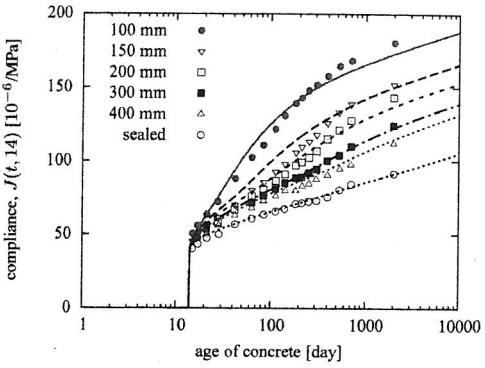

Figure 9. **Creep** compliance curves measured by Bryant and Vadhanavikkit (1987) on **drying slabs** of different thicknesses D and their fits by the **MPS model** with parameters $\mu_S = 2 \cdot 10^{-10}$/(MPa·day) and $\tilde{p} = 0.6$; onset of drying at $t_0 = 8$ days, loading applied at $t' = 14$ days.

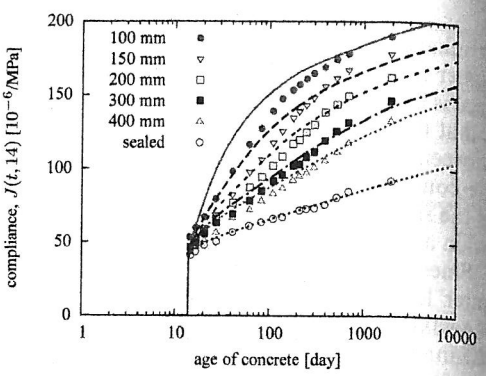

Figure 10. **Creep** compliance curves measured by Bryant and Vadhanavikkit (1987) on **drying prisms** of different sizes D and their fits by the **MPS model** with parameters $\mu_S = 2 \cdot 10^{-10}$/(MPa·day) and $\tilde{p} = 0.6$; onset of drying at $t_0 = 8$ days, loading applied at $t' = 14$ days.

modifying the exponent $\tilde{p}$, which is normally considered as fixed by the standard MPS theory. A slight reduction of this parameter from its default value $\tilde{p} = 2$ reduces the spurious (reverted) size effect on drying creep, and further reduction eventually produces the correct size effect. Of course, a change of $\tilde{p}$ must be accompanied by a recalibration of the fluidity parameter μ_S. It turns out that the best agreement with the experimental data of Bryant & Vadhanavikkit (1987) is obtained with $\tilde{p} = 0.6$ and $\mu_S = 2 \cdot 10^{-10}$/(MPa·day). This is true not only for the experiments on slabs (Fig. 9) but also for another set of experiments on prisms (Fig. 10).

Recall that exponent $\tilde{p}$ introduced in (14) was defined as $p/(p-1)$ where p is the original exponent of the MPS theory, used in (3) and (6). Unfortunately, the optimal value $\tilde{p} = 0.6$ obtained by pure numerical fitting of the size effect on drying creep corresponds to a negative value of p, namely $p = -1.5$. The original equations of the MPS theory would then lose their physical meaning. This motivates the need for a modification of the governing equations that can produce the correct size effect while retaining a reasonable physical meaning.

6 MODIFIED FORMULATION

The delay of drying creep behind the changes of humidity exhibited by the standard MPS theory can be attributed to the fact that the microprestress relaxation is governed by a single first-order differential equation, which posseses a certain characteristic time. No doubt, the microprestress relaxation process would be better described by a continuous relaxation spectrum covering a wide range of characteristic times, similar to what is needed for accurate modeling of the viscoelastic strain by the solidification theory. Since the microprestress cannot be directly measured, it would be next to impossible to determine the details of its relaxation spectrum in a reliable manner. Therefore, as a partial remedy, it is suggested to capture at least the "almost instantaneous" part of the effect of humidity change on viscosity by a separate rheologic unit. Analogous adjustments could be done for the effect of temperature changes but in this preliminary study we focus on the case of variable humidity but constant temperature.

The main idea of the modified MPS model is to split the viscous dashpot that represents the creep flow into two dashpots linked in series, one of them corresponding to basic creep and the other to drying creep. Due to the serial coupling, the total fluidity

$$\frac{1}{\eta} = \frac{1}{\eta_1} + \frac{1}{\eta_2} \tag{21}$$

is the sum of the partial fluidities (reciprocal values of viscosities η_1 and η_2). The part that corresponds to basic creep should agree with the B3 model, and thus

$$\frac{1}{\eta_1} = \frac{q_4}{t} \tag{22}$$

At constant humidity, the additional fluidity due to drying creep flow should vanish. At variable humidity, it can be related to the rate of pore relative humidity, e.g. by setting

$$\frac{1}{\eta_2} = \frac{k_2 q_4}{t} \left| \dot{f} \right| \tag{23}$$

where k_2 is a parameter controlling the magnitude of drying creep and f is a certain function of pore relative humidity h. According to this formula,

the additional fluidity (which then results into an additional creep strain) is generated by changes of humidity, and disappears as soon as the humidity ceases to vary. This is different from the original MPS concept, according to which changes of humidity generate additional microprestress and this effect is felt even after the humidity ceases to vary, until it gradually relaxes.

Numerical simulations indicate that the best agreement with experimental data is obtained with

$$f(h) = \ln h \tag{24}$$

and with the actual time t in (23) replaced by the equivalent time t_e, which "runs" more slowly at lower humidities. Equation (23) then takes the form

$$\frac{1}{\eta_2} = \frac{k_2 q_4}{t_e} \left| \frac{\dot{h}}{h} \right| \tag{25}$$

After this modification, creep of drying slabs of different thicknesses is captured very well (Fig. 11). For prisms, some deviation from the experimental results can be observed (Fig. 12), but the results are still substantially better that with the original MPS theory. The resulting size effect on drying creep is qualitatively correct, and the spurious delay of drying creep observed for the original MPS is eliminated. The compliance growth at early stages is even somewhat too fast. Note that the suggested modification of the MPS theory deals with a single parameter k_2, which controls the magnitude of drying creep and can be adjusted on one creep curve, measured for a specimen of one size. Simulation of the creep curves corresponding to other sizes can then be considered as a prediction. From this point of view, the agreement found in Figs. 11–12 for many curves computed with the same $k_2 = 90$ days is excellent.

A potential questionable point of the modified model could be the explicit dependence of viscosity η_2 on the age or equivalent age. In fact, this can be justified by placing the formulation into the framework of the original MPS theory, which was, at constant temperature $T = T_0$, based on the following equations:

$$\dot{S} + \psi_S c_0 S^p = k_1 T_0 \left| \frac{\dot{h}}{h} \right| \tag{26}$$

$$\frac{1}{\eta} = (p-1) c_0 q_4 S^{p-1} \tag{27}$$

In the absence of drying ($\dot{h} = 0$), and with a suitable initial condition, the resulting viscosity corresponds to η_1 given by (22). Now taking into account (21)–(23) and (25) and ignoring the

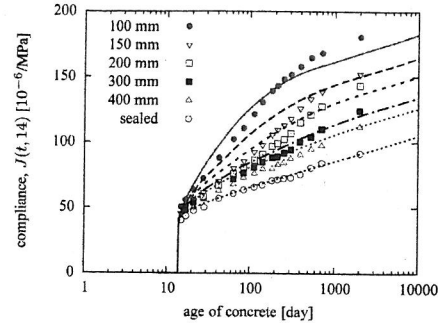

Figure 11. **Creep** compliance curves measured by Bryant and Vadhanavikkit (1987) on **drying slabs** of different thicknesses D and their fits by the **modified MPS model** with parameter $k_2 = 90$ days; onset of drying at $t_0 = 8$ days, loading applied at $t' = 14$ days.

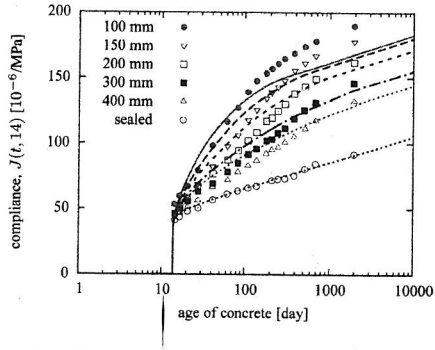

Figure 12. **Creep** compliance curves measured by Bryant and Vadhanavikkit (1987) on **drying prisms** of different sizes D and their fits by the **modified MPS model** with parameter $k_2 = 90$ days; onset of drying at $t_0 = 8$ days, loading applied at $t' = 14$ days.

difference between t and t_e, we find that the modified formulation can be described by

$$\dot{S} + c_0 S^p = 0 \tag{28}$$

$$\frac{1}{\eta} = (p-1) c_0 q_4 S^{p-1} \left(1 + k_2 \left| \frac{\dot{h}}{h} \right| \right) \tag{29}$$

So the effect of variable humidity is moved from the right-hand side of the equation for microprestress relaxation to the expression linking the current viscosity to the microprestress. The microprestress is used just for theoretical justification but does not actually need to be computed because the microprestress relaxation equation (28) has a known analytical solution, valid even under variable humidity. One could even consider a more general model in which the terms dependent on the humidity rate would appear both on the right-hand side of the microprestress relaxation equation (26) and in the expression for viscosity (29), thus accounting for both instantaneous and delayed effects.

7 CONCLUSION

The governing differential equation of the microprestress-solidification theory has been rewritten in terms of viscosity. The microprestress, which cannot be directly measured, has been completely eliminated from the formulation. This formal rearrangement has permitted a reduction of the number of model parameters, keeping the constitutive behavior equivalent to the original theory. An efficient and accurate numerical algorithm has been derived (Jirásek & Havlásek 2014) and implemented into the OOFEM finite element package, which can be used for simulations of concrete creep at variable temperature and humidity.

A comparison of the results of numerical simulations to experimental data of Fahmi, Polivka, & Bresler (1972) has shown that the original MPS theory performs well for load levels within the linear range of creep if the temperature is increased and reduced in one cycle, provided that the parameters are properly adjusted. For repeated temperature cycles, the effect of variable temperature on creep is overestimated, as discussed in detail in another publication (Jirásek & Havlásek 2014).

The main focus of the present paper has been on the size effect on drying creep. Numerical simulations of the tests reported by Bryant & Vadhanavikkit (1987) have revealed that, with the standard value of exponent $\tilde{p} = 2$ that appears in the viscosity evolution equation and is uniquely linked to the original exponent p of the MPS theory, the increase of compliance due to drying creep is delayed with respect to the experimental data and exhibits the opposite size effect. The correct size effect can be recovered with a nonstandard value of exponent $\tilde{p} = 0.6$, which corresponds to a negative value $p = -1.5$ of the original exponent. This is unfortunately nonphysical. As an alternative remedy, a modified MPS theory has been proposed, with an additive split of fluidity into two terms representing the contributions of viscous flow to basic creep and to drying creep. The suggested modification uses a single parameter that controls the magnitude of drying creep. Good fits of the experimental data of Bryant & Vadhanavikkit (1987) measured on slabs and prisms of five different sizes have been constructed with a fixed value of this parameter.

ACKNOWLEDGMENTS

Financial support provided to the second and third author by the Czech Science Foundation under projects P105/10/2400 and 13–18652S is gratefully acknowledged.

REFERENCES

Bažant, Z.P. (1995). Creep and damage in concrete. In J. Skalny and S. Mindess (Eds.), *Materials Science of Concrete IV*, pp. 355–389. Westerville, OH: Am. Ceramic. Soc.

Bažant, Z.P. & S. Baweja (1995). Creep and shrinkage prediction model for analysis and design of concrete structures –model B3. *Materials and Structures 28*, 357–365. RILEM Recommendation, in collaboration with RILEM Committee TC 107-GCS, with Errata, Vol. 29 (March 1996), p. 126.

Bažant, Z.P., G. Cusatis, & L. Cedolin (2004). Temperature effect on concrete creep modeled by microprestress-solidification theory. *Journal of Engineering Mechanics, ASCE 130*, 691–699.

Bažant, Z.P., A.P. Hauggaard, & S. Baweja (1997). Microprestress solidification theory for concrete creep. II: Algorithm and verification. *Journal of Engineering Mechanics, ASCE 123*, 1195–1201.

Bažant, Z.P., A.P. Hauggaard, S. Baweja, & F.J. Ulm (1997). Microprestress solidification theory for concrete creep. I: Aging and drying effects. *Journal of Engineering Mechanics, ASCE 123*, 1188–1194.

Bažant, Z.P. & L.J. Najjar (1971). Drying of concrete as a nonlinear diffusion problem. *Cement and Concrete Research 1*, 461–473.

Bažant, Z.P. & S. Prasannan (1989a). Solidification theory for concrete creep: I. Formulation. *Journal of Engineering Mechanics, ASCE 115*, 1691–1703.

Bažant, Z.P. & S. Prasannan (1989b). Solidification theory for concrete creep: II. Verification and application. *Journal of Engineering Mechanics, ASCE 115*, 1704–1725.

Bryant, A.H. & C. Vadhanavikkit (1987). Creep, shrinkage-size, and age at loading effects. *ACI Materials Journal 84*, 117–123.

Fahmi, H.M., M. Polivka, & B. Bresler (1972). Effect of sustained and cyclic elevated temperature on creep concrete. *Cement and Concrete Research 2*, 591–606.

Fédération internationale de béton (*fib*) (2010). *Draft of fib Model Code*. Lausanne, Switzerland.

Havlásek, P. & M. Jirásek (2012). Modeling of concrete creep based on microprestress-solidification theory. *Acta Polytech-nica 52*, 34–42.

Jirásek, M. & P. Havlásek (2014). Microprestress-solidification theory of concrete creep: Reformulation and improvement. *Cement and Concrete Research*. Submitted for review.

Kommendant, G.J., M. Polivka, & D. Pirtz (1976). Study of concrete properties for prestressed concrete reactor vessels. part 2: Creep and strength characteristics of concrete at elevated temperatures. Technical Report UC SESM 76–3, Department of Civil Engineering, University of California, Berkeley, Cal-ifornia.

Nasser, K.W. & A.M. Neville (1965). Creep of concrete at elevated temperatures. *ACI Journal 62*, 1567–1579.

Patzák, B. (2012). OOFEM – an object-oriented simulation tool for advanced modeling of materials and structures. *Acta Polytechnica 52*, 59–66.

Patzák, B. & Z. Bittnar (2001). Design of object oriented finite element code. *Advances in Engineering Software 32*, 759–767.